

## Comparison Between Terrestrial Laser Scanning and Close Range Photogrammetry for Three-Dimensional Modeling

Ateaya B Azeez<sup>1</sup>, Ahmed M Amin<sup>2</sup>, Ahmed I El-Hattab<sup>3</sup> and Ahmed A El-sharkawy<sup>4</sup>

### Abstract

Recently, the generation of three-dimensional photo-realistic models has been one of the most interesting topics in photogrammetry and LiDAR. The purpose of this research was to study, compare, and assess the use of close-range photogrammetry and terrestrial laser scanning techniques to reconstruct 3D objects. The two façades of Shorouk Building were chosen in this study. The results indicated that terrestrial laser scanning technique was accurate enough for precise three dimensional applications. The same results were obtained by close-range photogrammetry technique. For wide façades, it is important to divide the facade into several parts for the purpose of achieving high accuracy in CRP technique and each division is considered as a separate façade.

**Keywords:** *Close Range Photogrammetry; Terrestrial Laser Scanning; Modelling.*

### 1. Introduction

Close Range Photogrammetry (CRP) and Terrestrial Laser Scanning (TLS) are two typical techniques used to reconstruct 3D objects [1]. Both techniques enable the collection of 3D points. However, due to specific requirements in different reconstruction projects and the different characteristics of both methods, none of these technologies is superior over the other [2]. The purpose of this research was to study, compare, and assess the use of close-range photogrammetry and terrestrial laser scanning techniques to reconstruct 3D objects [3].

### 2. Practical Work

#### 2.1. Study Area

The location of study was chosen to be in El Shorouk Academy, which is a private educational academy located in El Shorouk city some 35 km east of Cairo. Two façades of the Higher Institute for Engineering Education buildings were selected.

#### 2.2. Total Station Measurements

To study both façades of The Shorouk building, it is required to observe number of points using total station instrument. Some of these points were used as Ground

Control Points (GCPs) and the rest were used as check points (CHPs) to evaluate the used equipment and processing technique. The coordinates (X, Y, and Z) of these points were observed using (SET-X Sokkia) total station and the measurements were made using reflectorless technique

For The first façade, a set of points were fixed on the façade according to its extent and geometry. Thirty points were selected to be observed; ten of these points were referred to GCPs (numbers 2, 5, 7, 10, 12, 18, 19, 21, 27 and 28) and the rest were used as CHPs. Figure 1 illustrates the location of GCPs and CHPs in the first façade.

Regarding, the second facade, twenty-eight points were selected to be observed; ten of these points were referred to GCPs (numbers 2, 6, 9, 10, 11, 17, 22, 23, 25 and 13) and the rest were considered CHPs. Figure 2 illustrates the location of GCPs and CHPs in the second façade.

#### 2.3. CRP Technique

In this research, the Multi-photo orientation used as a method of recovering the photographic configuration of photo assembly. This method Designed for determining camera stations and object points sequentially by intersection and resection model [4].

##### 2.3.1. Images Capturing

Every façade was divided into two parts due to the large width of the facade. For every part, three camera exposure stations were set out in front of the façade. Two images were taken in the middle to connect the two parts together.

The used capture device was a hand-held Rolleiflex 6008 camera [5]. The camera output was a hard copy format (negative of 60x60 mm), which was converted into a digital format for further processing. Digital images

<sup>1</sup>Researcher & Head of Land Surveying Department, National Authority for Remote Sensing and Space Sciences, Egypt, E-mail: [Ateayabekheet@gmail.com](mailto:Ateayabekheet@gmail.com)

<sup>2</sup>Professor of Surveying and Photogrammetry, Faculty of Engineering, Suez Canal University, Ismailia, Egypt, E-mail: [Profahmedamin@yahoo.com](mailto:Profahmedamin@yahoo.com)

<sup>3</sup>Professor of Surveying and Geodesy, Faculty of Engineering, Port Said University, Port Said, Egypt, E-mail: [Dr.ahmed.elhattab@gmail.com](mailto:Dr.ahmed.elhattab@gmail.com)

<sup>4</sup>Assistant lecturer & PhD student at Civil Eng. Dept., Faculty of Engineering, Port Said University, port said, Egypt, E-mail: [Eng.ahmed.sharkawy@gmail.com](mailto:Eng.ahmed.sharkawy@gmail.com)

data were derived from the frame images of photographic film by using high-precision photogrammetric scanner (AGFA DUE SCAN scanner with resolution 4000 dpi).

### 2.3.2. Data Processing

Close Range Digital Workstation (CDW) was used for data processing [6]. In fixing System, many trials had been conducted. These trials were three trials for 3 GCPs (located Once in the left part and once in the right part and once in the two parts), four trials for 4 GCPs (located Once in the left part and once in the right part and twice in the two parts) and one trial for each 5 GCPs, 6 GCPs, 7 GCPs, 8 GCPs, 9 GCPs and 10 GCPs (all of them located in the two parts).

When getting the report, the coordinates (X, Y, and Z) of the CHPs were obtained. These coordinates were

compared by the corresponding coordinates obtained by using total station.

$$E_X = X_{TS} - X_{CRP} \quad (1)$$

$$E_Y = Y_{TS} - Y_{CRP} \quad (2)$$

$$E_Z = Z_{TS} - Z_{CRP} \quad (3)$$

$$E_R = \sqrt{[(E_X)^2 + (E_Y)^2 + (E_Z)^2]} \quad (4)$$

$$RMS_E = \sqrt{\frac{\sum E^2}{n}} \quad (5)$$

Where ( $X_{CRP}$ ,  $Y_{CRP}$ , and  $Z_{CRP}$ ) are the coordinates of CHPs from CRP technique, ( $X_{TS}$ ,  $Y_{TS}$ , and  $Z_{TS}$ ) are the coordinates of CHPs from Total Station, ( $E_X$ ,  $E_Y$ , and  $E_Z$ ) are residual error of the coordinates,  $E_R$  is the resultant residual error, and  $n$  is the number of CHPs.

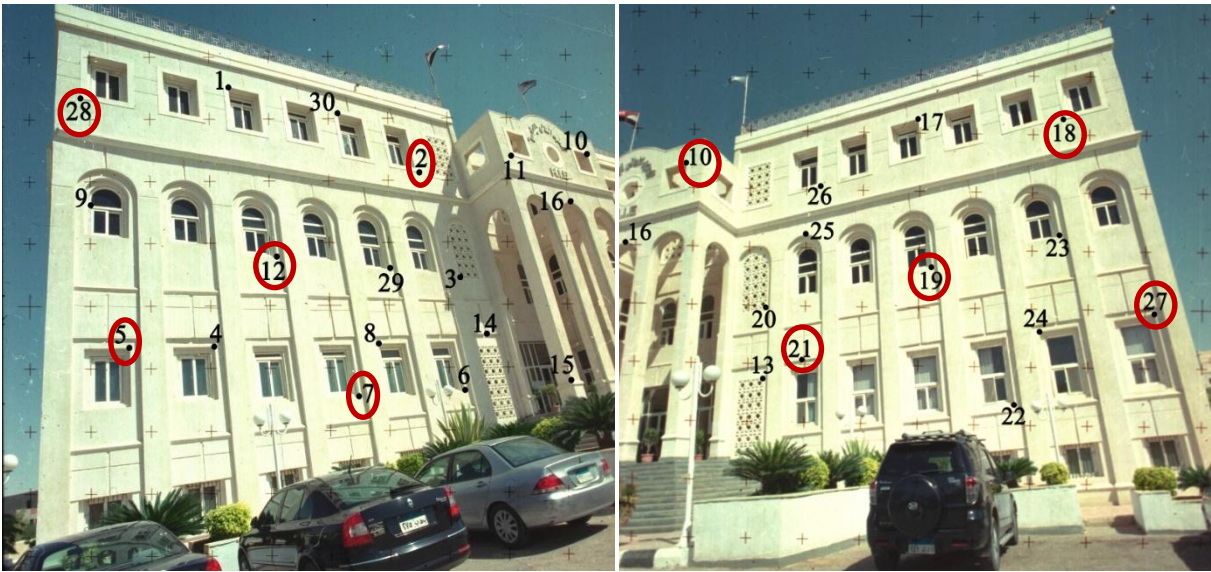


Figure 1: The location of GCPs and CHPs in the first façade (the two parts).

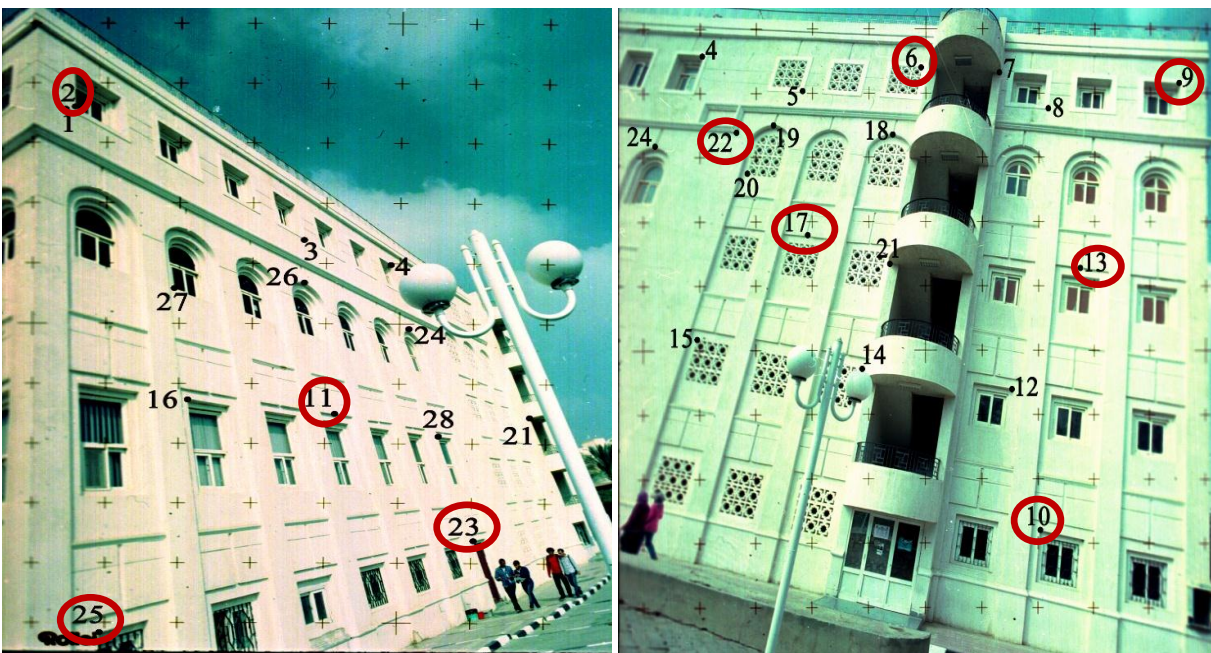


Figure 2: The location of GCPs and CHPs in the second façade (the two parts).

## 2.4. TLS Technique

The used IIRIS-HD scanner from Optech is considered a camera scanner [7]. Several scanning positions were chosen to cover the full façade because of the presence of obstructions which obscure the view. In every scan, the scanner divides the region of interest into several tasks - with overlapping between them- depending on the distance between the laser scanner and the object. All the captured raw data were converted from internal format (\*.asc) to the point cloud package format (\*.ixf) by using parser program.

### 2.4.1. Data Processing

The JRC-Reconstructore software package was used for point cloud processing [8]. The procedure of point cloud processing was importing the point cloud grids to the project and applying Grid pre-processing to every task.

As every scan position consisted of more than one point cloud, Iterative Closest Point Registration (ICP) was needed. ICP registration is an algorithm to perform automatically fine registration for the purpose of moving point cloud towards one or more reference clouds with overlap between them. The algorithm finds points on the moving cloud that are close to the reference clouds.

Every grid point cloud has to be aligned with the others grid point cloud. The pre-registration technique allows manually computes a rough alignment between two grid point clouds. The pre-registration procedure works by finding three couples of corresponding points among the reference and moving grids. The alignment can be later refined automatically, using ICP registration.

Then, conduct Georeference for all point clouds by using a list of reference points. In this step the GCPs were determined to be used in Georeference. Then the CHPs were determined in the points cloud to get their coordinates (X, Y, and Z). These coordinates were compared by the corresponding coordinates obtained by using the total station.

$$E_X = X_{TS} - X_{LS} \quad (6)$$

$$E_Y = Y_{TS} - Y_{LS} \quad (7)$$

$$E_Z = Z_{TS} - Z_{LS} \quad (8)$$

$$E_R = \sqrt{[(E_X)^2 + (E_Y)^2 + (E_Z)^2]} \quad (9)$$

$$RMS_E = \sqrt{\frac{\sum E^2}{n}} \quad (10)$$

Where ( $X_{LS}$ ,  $Y_{LS}$ , and  $Z_{LS}$ ) are the coordinates of CHPs from TLS technique, ( $X_{TS}$ ,  $Y_{TS}$ , and  $Z_{TS}$ ) are the coordinates of CHPs from Total Station, ( $E_X$ ,  $E_Y$ , and  $E_Z$ )

are Residual error of the coordinates,  $E_R$  is the resultant Residual error, and  $n$  is the number of CHPs.

## 3. Results and Analysis

### 3.1. CRP Technique

Tables 1 and 2 indicate the results for all trials when using CRP Technique in the two façades. Figures 3 and 4 showed the RMS resultant residual error for all trials. When specify three or four GCPs in one part of the façade, a great error had appeared in the CHPs coordinates. When specify three or four GCPs in the two parts of the façade, an improvement has appeared in the CHPs coordinates. Any increase in the number of GCPs to eight points achieved the best results accuracy. On the other side, any increase in the number of GCPs more than eight did not achieve any significant impact.

Table 1: The RMS residual error results when using CRP technique for First Façade

	RMS (mm)			
	X	Y	Z	R
3 GCPs left	26.39	41.37	57.07	75.27
3 GCPs right	31.84	62.29	22.21	73.40
3 GCPs two	21.73	35.86	18.65	45.89
4 GCPs left	14.61	21.52	41.87	49.29
4 GCPs right	28.87	59.93	22.15	70.11
4 GCPs two	13.36	36.74	5.64	39.50
4 GCPs two	15.89	28.82	6.43	33.53
5 GCPs	14.84	23.72	6.75	28.78
6 GCPs	13.50	19.04	5.15	23.90
7 GCPs	9.67	9.25	6.15	14.73
8 GCPs	7.47	8.76	4.02	12.19
9 GCPs	8.29	8.50	4.13	12.57
10 GCPs	8.55	8.38	4.25	12.70

Table 2: The RMS residual error results when using CRP technique for First Façade

	RMS (mm)			
	X	Y	Z	R
3 GCPs left	90.82	22.43	15.99	94.91
3 GCPs right	22.70	99.87	21.02	104.55
3 GCPs two	12.84	40.38	48.23	64.20
4 GCPs left	28.69	19.37	19.86	39.91
4 GCPs right	28.65	103.41	17.65	108.75
4 GCPs two	28.92	24.27	8.15	38.62
4 GCPs two	24.82	24.52	10.60	36.47
5 GCPs	13.86	16.13	11.75	24.30
6 GCPs	12.94	13.98	8.86	21.01
7 GCPs	10.23	12.35	6.44	17.28

8 GCPs	10.10	8.42	6.11	14.50
9 GCPs	10.22	8.81	6.21	14.85

10 GCPs	10.27	8.81	6.21	14.89
---------	-------	------	------	-------

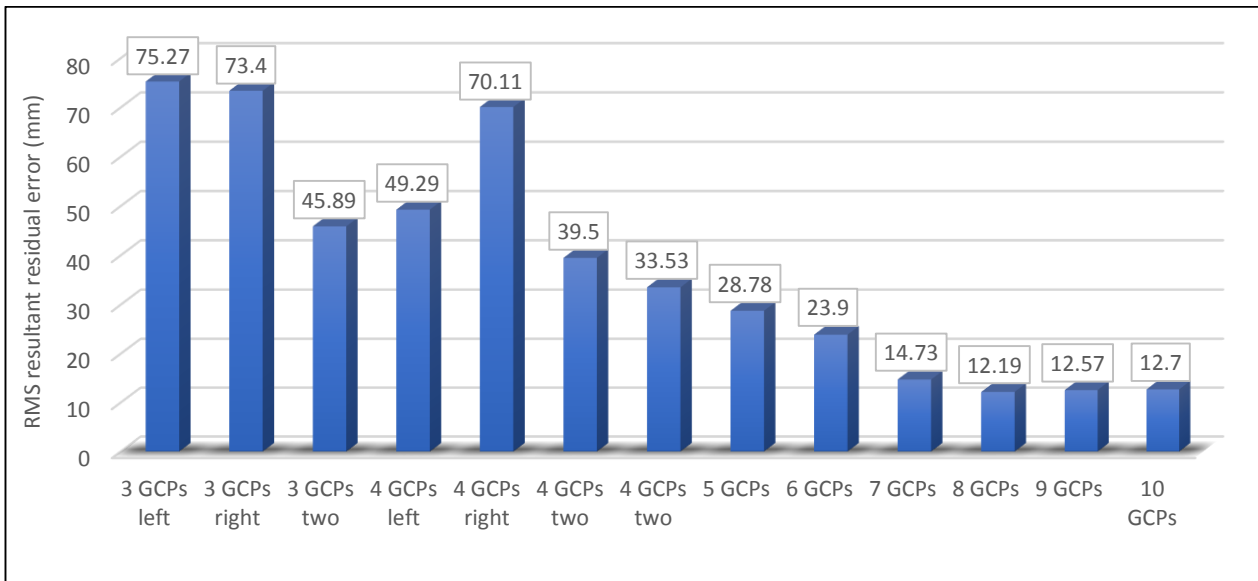


Figure 3: The RMS residual errors in CRP technique for the First Façade of Shorouk building.

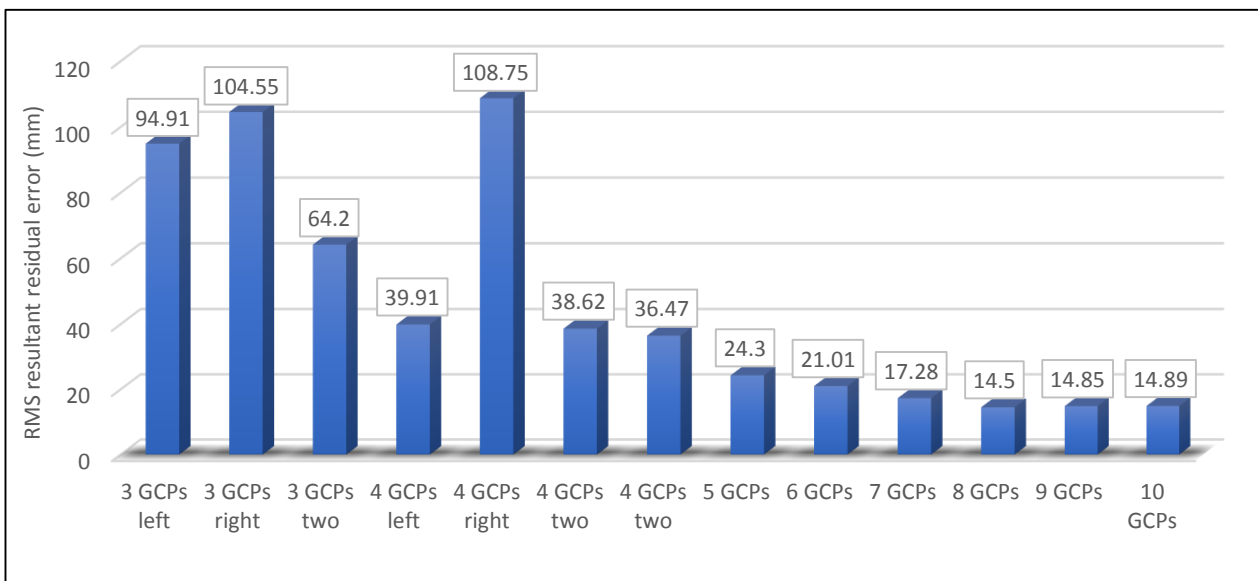


Figure 4: The RMS residual errors in CRP technique for the Second Façade of Shorouk building.

### 3.2. TLS Technique

Tables 3 and 4 illustrate the results of using TLS technique on CHPs coordinates for the two facades. These coordinates were compared with the corresponding CHPs coordinates obtained by the total station. Then the residual error was calculated for all the coordinates. The calculations of the RMS residual error and the maximum residual error were also shown in these tables. These results of TLS Technique indicate that RMSE was found to be in the range of 11 to 12 mm.

Table 3: The results of applying TLS technique in the First Facade.

Points	X <sub>LS</sub> (m)	Y <sub>LS</sub> (m)	Z <sub>LS</sub> (m)	X <sub>TS</sub> (m)	Y <sub>TS</sub> (m)	Z <sub>TS</sub> (m)	E <sub>X</sub> (m)	E <sub>Y</sub> (m)	E <sub>Z</sub> (m)	E <sub>R</sub> (m)
1	721.976	878.391	17.295	721.972	878.399	17.300	0.004	-0.008	-0.005	0.010
3	730.015	873.105	10.307	730.011	873.113	10.306	0.004	-0.008	0.001	0.009
4	721.121	879.253	7.556	721.125	879.267	7.556	-0.004	-0.014	0.000	0.014
6	729.010	873.807	5.679	729.004	873.810	5.682	0.006	-0.003	-0.003	0.007
8	725.999	875.853	7.560	725.998	875.864	7.562	0.001	-0.011	-0.002	0.012
9	718.421	881.386	11.972	718.420	881.399	11.975	0.001	-0.013	-0.003	0.013
11	730.315	869.666	14.854	730.304	869.654	14.854	0.011	0.012	0.000	0.016
13	738.790	867.012	7.355	738.796	867.015	7.367	-0.006	-0.003	-0.012	0.013
14	730.487	872.678	7.852	730.475	872.671	7.850	0.012	0.007	0.002	0.014
15	729.885	870.052	5.270	729.870	870.048	5.271	0.015	0.004	-0.001	0.016
16	733.040	867.843	13.077	733.030	867.843	13.070	0.010	0.000	0.007	0.012
17	744.620	862.764	17.320	744.614	862.756	17.323	0.006	0.008	-0.003	0.010
20	738.795	866.983	10.259	738.801	866.985	10.258	-0.006	-0.002	0.001	0.006
22	746.685	861.507	5.320	746.688	861.515	5.323	-0.003	-0.008	-0.003	0.008
23	748.671	860.185	10.900	748.684	860.182	10.900	-0.013	0.003	0.000	0.013
24	747.655	860.866	7.633	747.655	860.881	7.636	0.000	-0.015	-0.003	0.015
25	740.315	865.791	13.101	740.314	865.776	13.101	0.001	0.015	0.000	0.015
26	740.869	865.351	15.214	740.869	865.359	15.217	0.000	-0.008	-0.003	0.008
29	727.001	875.148	10.438	726.998	875.142	10.436	0.003	0.006	0.002	0.007
30	725.913	875.685	17.301	725.916	875.692	17.299	-0.003	-0.007	0.002	0.008
RMS Of E (mm)							6.98	8.68	3.60	11.70
Max. E (mm)							15.39	15.31	11.60	16.37

Table 4: The results of applying TLS technique in the Second Facade.

Points	X <sub>LS</sub> (m)	Y <sub>LS</sub> (m)	Z <sub>LS</sub> (m)	X <sub>TS</sub> (m)	Y <sub>TS</sub> (m)	Z <sub>TS</sub> (m)	E <sub>X</sub> (m)	E <sub>Y</sub> (m)	E <sub>Z</sub> (m)	E <sub>R</sub> (m)
1	751.641	858.753	15.500	751.649	858.746	15.492	-0.008	0.007	0.008	0.013
3	756.639	866.006	15.537	756.645	866.002	15.538	-0.006	0.004	-0.001	0.007
4	760.621	871.785	17.385	760.623	871.789	17.379	-0.002	-0.004	0.006	0.008
5	763.530	875.880	15.910	763.519	875.881	15.913	0.011	-0.001	-0.003	0.011
7	768.358	881.880	16.621	768.348	881.880	16.624	0.010	0.000	-0.003	0.010
8	768.900	883.751	15.967	768.892	883.757	15.969	0.008	-0.006	-0.002	0.010
12	768.630	883.765	6.555	768.637	883.769	6.552	-0.007	-0.004	0.003	0.009
13	769.710	885.160	10.445	769.710	885.155	10.459	0.000	0.005	-0.014	0.015
14	765.840	879.840	6.457	765.851	879.827	6.460	-0.011	0.013	-0.003	0.018
15	762.585	874.885	6.471	762.575	874.879	6.471	0.010	0.006	0.000	0.011
16	753.000	860.988	7.610	753.016	860.989	7.610	-0.016	-0.001	0.000	0.016
18	765.782	879.241	14.455	765.785	879.252	14.455	-0.003	-0.011	0.000	0.012
19	763.007	875.170	14.446	762.997	875.175	14.440	0.010	-0.005	0.006	0.013
20	762.565	874.825	12.467	762.553	874.826	12.461	0.012	-0.001	0.006	0.014
21	766.844	879.689	9.393	766.844	879.681	9.393	0.000	0.008	0.000	0.008
24	760.280	871.316	13.139	760.284	871.318	13.126	-0.004	-0.002	0.013	0.014
26	756.240	865.447	13.112	756.242	865.450	13.114	-0.002	-0.003	-0.002	0.004
28	759.787	870.881	7.599	759.797	870.869	7.595	-0.010	0.012	0.004	0.016
RMS Of E (mm)							8.55	6.50	5.80	12.20
Max. E (mm)							16.46	12.89	13.94	17.51

## 4. Conclusions

The following results may be concluded:

- When using TLS technique, the RMSE was found to be in the range of 11 to 12 mm. but when using CRP technique, the RMSE was found to be in the range of 12 to 14 mm. The obtained results are acceptable for precise three dimensional applications.
- For wide facades, it is important to divide the facade into several parts for the purpose of achieving high accuracy in CRP technique. In this case, each division is considered as a separate façade and four GCPs - well distributed - are required for each division.

## 5. References

- [1] **Fritsch D, Khosravani AM, Cefalu A, and Wenzel K.**, “Multi-Sensors and Multi-Ray Reconstruction for Digital Preservation in Photogrammetric” Week '11, Ed. D., Wichmann, Berlin/Offenbach; pp. 305-323, 2011.
- [2] **Moussa, W.**, “Integration of digital photogrammetry and terrestrial laser scanning for cultural heritage data recording”, Verlag der Bayerischen Akademie der Wissenschaften in Kommission beim Verlag C.H.Beck, Studgart, Germany, 2014.
- [3] **Ahmed A El-Sharkawy, Ateaya B Azeez, Ahmed M Amin, and Ahmed I El-Hattab**, “Accuracy of Modern Three-Dimensional Data Acquisition Systems for The Restoration of Historical Buildings ”, A PhD thesis, Faculty of engineering, Port Said University, 2017.
- [4] **Luhman T., Robson S., Kyle S., and Boehm J.**, “Close Range Photogrammetry and 3D Imaging”, (2 ed.). Berlin, Germany: Walter de Gruyter GmbH, 2014.
- [5] **Rollei**, “Rollei-flex6008 User’s Manual”, Rollei Foto-Technic GmbH & Co KG Slazdahlumer Stress 196, D-38126 Braunschweig, Germany, 1993.
- [6] **Rollei**, “Rollei Digital Workstation User’s Manual”, Rollei Foto-Technic GmbH& Co KG Slazdahlumer Stress 196, D-38126 Braunschweig, Germany, 1996.
- [7] **Optech**, “ILRIS Operation Manual”, Optech Incorporated Industrial & 3D Imaging Division, Vaughan, Ontario, Canada, 2009.
- [8] **Gexcel**, “JRC 3D Reconstructor® User Manual”, Gexcel Srl. Geomatics & Excellence - A University of Brescia Spin Off Company, Brescia, Italy, 2012.